

Extended state observer based smooth switching control for tilt-rotor aircraft

ZOU Yiru¹, LIU Chunsheng^{1,*}, and LU Ke^{1,2}

1. School of Automation Engineering, Nanjing University of Aeronautics and Astronautics, Nanjing 211100, China;

2. Science & Technology on Rotorcraft Aeromechanics Laboratory, China Helicopter Research and Development Institute, Jingdezhen 333001, China

Abstract: A tilt-rotor aircraft has three flight modes: helicopter mode, airplane mode and conversion mode. Unlike the traditional aircraft, the tilt-rotor aircraft, which combines the characteristics of helicopters and fixed-wing aircraft, is a complex multi-body system with the violent variation of the aerodynamic parameters. For these characteristics, a new smooth switching control scheme is provided for the tilt-rotor aircraft. First, the reference commands for airspeed and nacelle angles are calculated by analyzing the conversion corridor and the conversion path. Subsequently, based on the finite-time switching theorem, an average dwell time condition is designed to guarantee the stability in the switching process. Besides, considering the state vibrations and bumps may appear in switching points, the fuzzy weighted logic is employed to improve the system transient performance. For disturbance rejection, three extended state observers are designed separately to estimate the disturbances in the switched systems. Compared with the traditional auto disturbance rejection control and proportion integration differentiation control, this method overcomes the conservatism of wasting the whole model information. The control performances of robustness and smoothness are verified with simulation, which shows that the new smooth switching control scheme is more targeted and superior than the traditional design method.

Keywords: tilt-rotor aircraft, switching control, extended state observer (ESO), smooth switching.

DOI: 10.23919/JSEE.2020.000025

1. Introduction

Unlike the traditional aircraft, a tilt-rotor aircraft can change its configuration by tilting the nacelle, and it provides a variety of flight characteristics as it converts from the helicopter mode to the aircraft mode [1,2]. It is for this reason that it can enhance civil or military transportation. However, the disadvantages are also unavoidable. First,

the flight dynamic of the tilt-rotor aircraft is much more complex than that of the traditional flight vehicles. Meanwhile, the system suffers from high interference when the aerodynamic configuration changes [3].

There are so many control schemes applied to tilt-rotor aircraft. In [4], the flight control law of a tilt-rotor aircraft was designed with the help of the inner/outer loop control structure. In [5], the nonlinear trajectory tracking controller for a tilt-rotor unmanned aerial vehicle (UAV) was designed using the dynamic model inversion technique integrated with the adaptation of neural networks. In [6], based on an optimal control concept, an online optimization control method was developed for the tilt-rotor UAV.

However, due to the violent aerodynamic change in tilt-rotor aircraft, a single controller may not satisfy the control precision, stability, reliability and other requirements of this complex flight system [7]. To solve this problem, a common multi-modes control scheme was proposed as the gain scheduling method [8]. The author developed a gain scheduling method for the tilt-rotor aircraft altitude control in [9], whereby the tilt-rotor frame pitch angle was selected as the scheduled variable of the off-line controller. Kong et al. [10] designed the classical proportion integration differentiation (PID) for the vertical flight stage and the backstepping controller for the transition flight. The two controllers are scheduled by the flight trajectory. Although the gain scheduling method is attractive, it may not guarantee the stability in the switching process, not to say the required performance over the full operating envelope of the system [11].

In such cases, drawing the lessons from the multi-model switching idea in [12,13], the author designed a multi-modes adaptive control for the tilt-rotor aircraft in [7]. However, this nonlinear switching control algorithm neglects the rotor inflow dynamic characteristic, which is computed by the iteration calculation in the practical flight

Manuscript received March 22, 2019.

*Corresponding author.

This work was supported by the Aeronautical Science Foundation of China (20175752045).

process [14]. For this reason, it is difficult to simply implement some traditional nonlinear control methods to the tilt-rotor aircraft, which are based on the exact feedback linearization technique.

To deal with the mentioned problem, recently, some researchers focus on utilizing some novel multi-modes control algorithms on tilt-rotor aircraft. Sun et al. [15] proposed the switching conditions to maintain the stability of the tilt-rotor aircraft switching process. To further facilitate the practical use of the gain scheduling method in the transition process of the tilt-rotor aircraft, Lu et al. [16] studied the developed gain scheduling algorithms based on the corrected generalized corridor. However, owing to the reason that the tilt-rotor aircraft needs to track different velocity signals with the nacelle tilting in the conversion corridor, the mentioned multi-modes control algorithms lead to two hidden troubles. First, the transition process of the tilt-rotor is unsmooth within the conversion corridor. Besides, the sudden switch may make the control signal jump in the switching point, which will bring the undesirable transient responses named bump [17]. The bump will activate the high-frequency dynamic characteristics that we have neglected in the small perturbations linearized method, which will further lead to mechanical damage, fatigue loading, or signal saturation [18].

In such cases, this paper can be inspired by smooth switching methods [19,20]. It is worth mentioning that, in these methods, the emergence of bumpless switching technique effectively reduces the control signal jumps and unsatisfactory performance caused by switching [21]. The idea of it is to force the output of the activated controller to be equal to the plant input at the switching time [22]. However, this method has a heavy computing burden, because it needs to calculate the system closed-loop dynamics between each off-line controller and bumpless transfer compensator in real time.

Besides, in the field of smooth switching, He et al. [19] developed the controllers for flexible airplane wing by minimizing the index of H_2 output performance and smoothness. Jiang et al. [23] was concerned with a systematic method of linear parameter varying (LPV) controller design for a morphing aircraft. Jiang et al. [24] designed the smooth switching control law based on the interpolation approach. But regrettably, although there are much progress made by the above literature, these methods have not been introduced to the research field of tilt-rotor aircraft yet, which causes the smooth transition control problem of this complex, changeable aircraft far from being solved.

Motivated by those mentioned above, a smooth switch-

ing controller based on the extended state observer (ESO) is proposed in this paper. The scheme of the smooth switching controller is novel in the sense that, based on the analysis of the conversion corridor, the conversion path is given. In contrast to the normal case, as the nacelle tilts, the transition of the tilt-rotor aircraft is a switch process with the sequence constraints. Thus, we propose a family of feedback stabilizing controllers as local controllers by satisfying the average dwell time (ADT) conditions. To reduce the bumps in the switching points, the flight states based fuzzy weighted strategy is employed as a measure for 'smoothness', which realizes the online calculation of the matching degree between the current dynamics and each sub-controller. In this way, it reconfigures the control law. For disturbance rejection, three ESO for each channel are respectively combined with this model-based control scheme, which avoids the waste of all the model information in the traditional auto disturbance rejection control (ADRC) technique [25,26].

By applying both the proposed control scheme and inner/outer loop based PID to the nonlinear tilt-rotor model, the simulation comparison results demonstrate that the stability, robustness and smoothness of the proposed method are more superior to those of the traditional PID.

2. Problem description

2.1 Nonlinear model of tilt-rotor aircraft

A tilt-rotor aircraft has three flight modes: helicopter mode, airplane mode and conversion mode. Table 1 shows the relationship between the nacelle angle β_M and different flight modes. During the conversion from the helicopter mode to the airplane mode, the flight mechanics (F_x, F_y, M_z) has complicated nonlinear mathematical relationships with the variables ($V_x, V_y, \omega_z, \theta, \delta_c, \delta_{long}, \delta_e, \beta_M$). For the details of aerodynamic forces calculation, one can refer to [27,28]. According to the above-cited modeling method, the complete nonlinear flight dynamic mathematical model of a tilt-rotor aircraft is built in the simulated environment of Matlab/Simulink, of which the primary purposes are: (i) to calculate the conversion corridor and the conversion path of the tilt rotor; (ii) to acquire the linear models in the trim points; (iii) to apply the control law to the nonlinear aircraft to verify the effect of the control law.

Remark 1 Considering the decoupling conditions in [29], this study decouples the longitudinal channel and the lateral channel for the convenience of design.

The formulation of the nonlinear model is briefly given as (1) for the completeness concern.

$$\dot{x} = f(x, u, \beta_M) =$$

$$\begin{bmatrix} -\omega_z V_y - g \sin \theta + \frac{F_x(\mathbf{x}, \mathbf{u}, \beta_M)}{m_B} \\ \omega_z V_x + g \cos \theta + \frac{F_y(\mathbf{x}, \mathbf{u}, \beta_M)}{m_B} \\ \frac{M_z(\mathbf{x}, \mathbf{u}, \beta_M)}{I_{yy}} \\ \omega_z \end{bmatrix} \quad (1)$$

where $\mathbf{x} = [V_x \ V_y \ \omega_z \ \theta]^T$ denotes the state vector; $\mathbf{u} = [\delta_c \ \delta_{long} \ \delta_e]^T$ denotes the input vector; I_{yy} denotes the rotational inertia; F_x and F_y denote the net forces along the X -axis and Y -axis in the Soviet body coordinate system; M_z is the pitch moment.

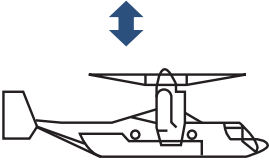
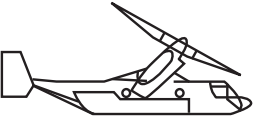
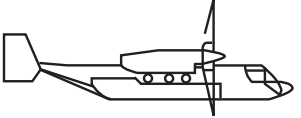
F_x , F_y and M_z can be described as

$$\begin{cases} F_x = F_{xR} + F_{xW} + F_{xF} + F_{xHT} + F_{xVT} \\ F_y = F_{yR} + F_{yW} + F_{yF} + F_{yHT} + F_{yVT} \\ M_z = M_{zR} + M_{zW} + M_{zF} + M_{zHT} + M_{zVT} \end{cases} \quad (2)$$

As a result, the whole flight longitudinal model is established.

Remark 2 In contrast to [30], this simulation model considers the effect of the rotor wake on the other aerodynamic surfaces and the nacelle tilting dynamics, so it is better to reflect the characteristics of large parameter changes caused by mode transition.

Table 1 Tilt-rotor aircraft at different flight modes

Mode	Helicopter mode	Conversion mode	Airplane mode
Rotor position			
Nacelle angle/(°)	90	$0 < \beta_M < 90$	0

2.2 Conversion corridor and conversion path

During the whole transition process, the desired motion is the one that can keep the altitude unchanged and drive the airspeed velocity to increase monotonically within the safe conversion corridor. As the nacelle tilts, the lower boundary of the conversion corridor is limited by wing stall, which means the tilt-rotor aircraft is not permitted flying with excessive low speed for fear of wing stall. The upper boundary of the conversion corridor is relative to engine power, the aircraft construction, etc.

All of the above limitations are considered in the modeling process. Thus, the conversion corridor can be obtained by the trim calculation, which is shown as Fig. 1.

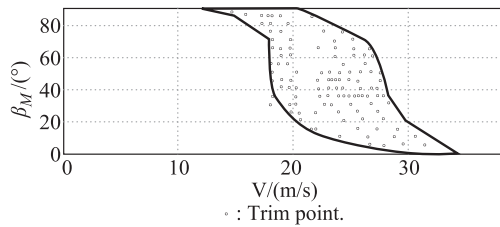


Fig. 1 Conversion corridor

Taking the conversion corridor into consideration, the conversion path is defined as below.

Definition 1 The conversion path S_{cp} is

$$\begin{cases} \beta_M = r(t), & t \in [T_0, T_f] \\ S_{cp} = f(\beta_M, V^*) \end{cases} \quad (3)$$

where $r(t)$ ($t \in [T_0, T_f]$) denotes the scheduling rule of the nacelle angle, which will be given in the simulation section; V^* is the corresponding airspeed, which can be divided into the horizontal component V_x and the vertical component V_y .

In general, there are so many possible tilting transition curves in the conversion corridor, as mentioned in [31], such as transition with a constant power or transition with a constant airspeed. The transition process in this paper aims at altitude maintenance, which demands that the reference value of V_y should always be zero to prevent falling. In addition, the pitch angle of the aircraft should make slow changes at low speeds. Satisfying the above requirements, the Gaussian function (4) is used to fit the curve of the conversion path, and the corresponding results can be seen in Fig. 2.

$$y = a_1 \cdot e^{-\left(\frac{x-b_1}{c_1}\right)^2} + a_2 \cdot e^{-\left(\frac{x-b_2}{c_2}\right)^2} + a_3 \cdot e^{-\left(\frac{x-b_3}{c_3}\right)^2} + a_4 \cdot e^{-\left(\frac{x-b_4}{c_4}\right)^2} + a_5 \cdot e^{-\left(\frac{x-b_5}{c_5}\right)^2} + a_6 \cdot e^{-\left(\frac{x-b_6}{c_6}\right)^2} \quad (4)$$

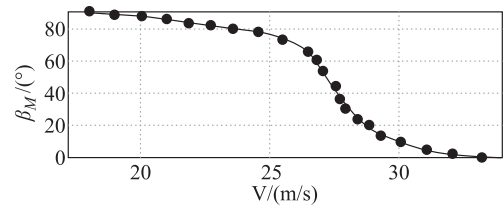


Fig. 2 Conversion path

Assume that the nonlinear system (1) is differentiable everywhere. We propose the linear model sets in the operation region by a perturbation method, which can be described as

$$\dot{\mathbf{x}} = \frac{\partial f}{\partial \mathbf{x}} \Big|_{[\mathbf{x}(\beta_M, V), \mathbf{u}(\beta_M, V)]} (\mathbf{x} - \mathbf{x}_\rho) + \frac{\partial f}{\partial \mathbf{u}} \Big|_{[\mathbf{x}(\beta_M, V), \mathbf{u}(\beta_M, V)]} (\mathbf{u} - \mathbf{u}_\rho). \quad (5)$$

where \mathbf{x}_ρ and \mathbf{u}_ρ denote the state vector and input vector in equilibrium points.

By setting $\frac{\partial f}{\partial \mathbf{x}} \Big|_{[\mathbf{x}(\beta_M, V), \mathbf{u}(\beta_M, V)]}$ as \mathbf{A}_ρ , $\frac{\partial f}{\partial \mathbf{u}} \Big|_{[\mathbf{x}(\beta_M, V), \mathbf{u}(\beta_M, V)]}$ as \mathbf{B}_ρ , the switched system of tilt-

rotor aircraft can be rewritten as

$$\dot{\mathbf{x}} = \mathbf{A}_\rho \mathbf{x} + \mathbf{B}_\rho \mathbf{u} + \mathbf{f}. \quad (6)$$

Based on the above mathematic model, three issues will be discussed in this paper.

Question 1 Construct the switching signal $\sigma(t)$ and the corresponding controllers to ensure the stability of the closed-loop system and the switching process.

Question 2 Improve the transient performance of the flight control system when the switching signals occur.

Question 3 Reduce the influence of the disturbance \mathbf{f} and enhance the robustness.

3. Controller design

The control structure is depicted in Fig. 3.

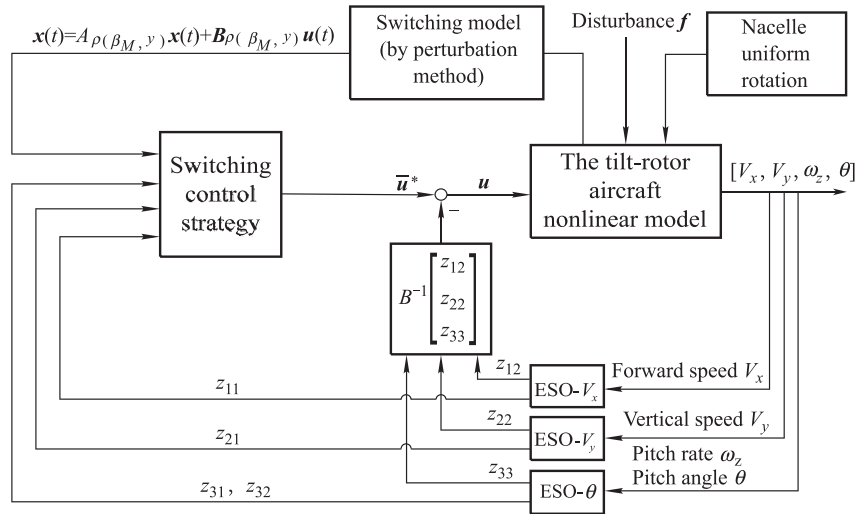


Fig. 3 Control structure

3.1 ESO design

As we know from the tilt-rotor nonlinear model (1), it is the airframe component that is disturbed by the external factors, which causes that the disturbance of the system is related to the aerodynamics F_x , F_y and M_z .

Based on these, the external disturbance \mathbf{f} is added to the states V_x , V_y and ω_z , which have direct mathematical relations with F_x , F_y and M_z in (1). In this paper, a class of disturbance \mathbf{f} satisfying the matching condition is considered, with the form of $\mathbf{B}_\rho \mathbf{d}$ as (13).

Then, we design three ESOs to observe the states and disturbances.

It can be derived that the ESO [32] for observing V_x is

$$\begin{cases} \dot{z}_{11} = z_{12} + \mathbf{A}_{\rho i} \mathbf{x} + \mathbf{B}_{\rho i} \mathbf{u} - 2\omega_{01}(z_{11} - V_x) \\ \dot{z}_{12} = -\omega_{01}^2(z_{11} - V_x) \end{cases}. \quad (7)$$

The ESO for observing V_y is

$$\begin{cases} \dot{z}_{21} = z_{22} + \mathbf{A}_{\rho j} \mathbf{x} + \mathbf{B}_{\rho j} \mathbf{u} - 2\omega_{02}(z_{21} - V_y) \\ \dot{z}_{22} = -\omega_{02}^2(z_{21} - V_y) \end{cases}. \quad (8)$$

The ESO for observing ω_z is proposed as

$$\begin{cases} \dot{z}_{31} = z_{32} - 3\omega_{03}(z_{31} - \theta) \\ \dot{z}_{32} = z_{33} + \mathbf{A}_{\rho k} \mathbf{x} + \mathbf{B}_{\rho k} \mathbf{u} - 3\omega_{03}^2(z_{31} - \theta) \\ \dot{z}_{33} = \omega_{03}^3(z_{31} - \theta) \end{cases}. \quad (9)$$

ω_{01} , ω_{02} and ω_{03} denote the observer bandwidth of the ESO. By choosing ω_{01} , ω_{02} and ω_{03} , the extended states can estimate the state variables, thus making the estimation errors converge to zero, i.e.,

$$\begin{cases} e_1 = z_{11} - V_x \rightarrow 0 \\ e_2 = z_{21} - V_y \rightarrow 0 \\ e_3 = z_{31} - \theta \rightarrow 0 \end{cases}. \quad (10)$$

Without loss of generality, we take the pitch angle ESO for example to analyze disturbance compensation. ω_z can be described as

$$\dot{\omega}_z = \mathbf{A}_{\rho k} \mathbf{x} + \mathbf{B}_{\rho k} \mathbf{u} + (0 \cdots e_k \cdots 0)^T f_3 \quad (11)$$

where $e_k = 1$, and f_3 is the total disturbance to be observed by the ESO of the pitch channel.

Subtracting (11) from (10), it yields

$$\dot{z}_{32} - \dot{\omega}_z = z_{33} - 3\omega_{03}^2(z_{31} - \theta) - f_3. \quad (12)$$

With the definition of the observer error ε as $\varepsilon = 3\omega_{03}^2(z_{31} - \theta) + (\dot{z}_{32} - \dot{\omega}_z)$, f_3 is expressed as $f_3 = z_{33} - \varepsilon$, the external interference f_3 approaches the extended state z_{33} when the ESO accurately estimates the aircraft state, namely,

$$z_{31} \rightarrow \theta, \dot{z}_{32} \rightarrow \dot{\omega}_z.$$

Similarly, the ESO for the forward channel and vertical channel can estimate not only the external disturbance f_2 and f_3 , but also the non-measurable state variables of the aircraft.

With the prior assumption

$$\begin{bmatrix} f_1 \\ f_2 \\ f_3 \end{bmatrix} = \begin{bmatrix} B_{\rho 11} & B_{\rho 12} & B_{\rho 13} \\ B_{\rho 21} & B_{\rho 22} & B_{\rho 23} \\ B_{\rho 31} & B_{\rho 32} & B_{\rho 33} \end{bmatrix} \begin{bmatrix} d_1 \\ d_2 \\ d_3 \end{bmatrix} = \begin{bmatrix} z_{12} \\ z_{22} \\ z_{33} \end{bmatrix} \quad (13)$$

the system can be rewritten as

$$\dot{\mathbf{x}} = \mathbf{A}_\rho \mathbf{x} + \mathbf{B}_\rho \mathbf{u} + \mathbf{f} = \mathbf{A}_\rho \mathbf{x} + \mathbf{B}_\rho (\mathbf{u} + \mathbf{d}). \quad (14)$$

Then, we design the control law as

$$\mathbf{u} = \bar{\mathbf{u}}^* - \mathbf{B}_\rho^{-1} \begin{bmatrix} z_{12} \\ z_{22} \\ z_{33} \end{bmatrix}. \quad (15)$$

It can be derived that the aircraft switching system under the disturbance \mathbf{f} turns into (16) after the interference compensation.

$$\dot{\mathbf{x}} = \mathbf{A}_\rho \mathbf{x} + \mathbf{B}_\rho \bar{\mathbf{u}}^* \quad (16)$$

3.2 Switching control design

Considering that the switching sequence of the tilt-rotor aircraft is restricted by the conversion path, the whole working regional \mathbf{X} can be divided into multiple overlapping sub-regions, in form of

$$\begin{cases} \Omega_1 \cup \cdots \cup \Omega_{\rho+1} \neq \emptyset \\ \rho = 1, \dots, N \end{cases}. \quad (17)$$

In this study, a set of feedback controllers are designed with concept of finite-time switching, which are in form of

$$\bar{\mathbf{u}} = \bar{\mathbf{K}}_{\sigma(t)} \mathbf{x}. \quad (18)$$

Adjacent controllers are switched according to the ADT logic. To reduce the states vibration in switching points, the control parameters scheduling module will be introduced later, which makes reference to the idea of fuzzy weighted.

The switching control module is depicted in Fig. 4.

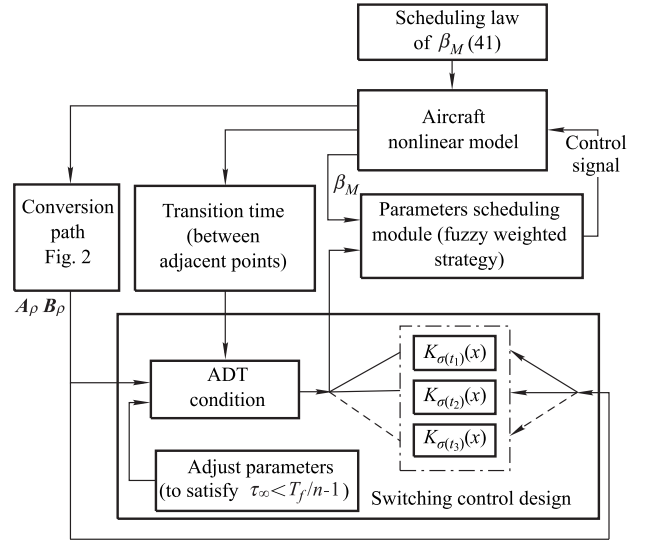


Fig. 4 Switching control module

In order to obtain the switching control law, the following definitions and lemmas are given.

Definition 2 [33] For the given positive constants c_1 and c_2 with $c_1 < c_2$, the switching signal $\sigma(t)$, the switching time T_f , and the positive definite matrix \mathbf{R} , the switching system (16) is said to be finite-time stabilization (FTS) with respect to $(c_1, c_2, T_f, \mathbf{R}, \sigma)$, for any $t \in [T_0, T_f]$ satisfying

$$\mathbf{x}^T(0) \mathbf{R} \mathbf{x}(0) \leq c_1 \Rightarrow \mathbf{x}^T(t) \mathbf{R} \mathbf{x}(t) < c_2. \quad (19)$$

Remark 3 The selection of the matrix \mathbf{R} has a close relation with the system performance, which will be explained in the simulation section.

Definition 3 [34] For each switching signal $\sigma(t)$, which satisfies $T_0 \leq t < T_f$, let $N_\sigma(t, T_f)$ denote the switching time of $\sigma(t)$ in the open interval (t, T_f) , and $T(t, T_f)$ denote the dwell time of each subsystem. For a given N_0 , $\tau > 0$, it denotes the set of all switching signals for which

$$N_\sigma(t, T_f) \leq N_0 + \frac{T_f(t, T)}{\tau_\alpha^*}. \quad (20)$$

The constant τ_α^* is called the ADT.

Lemma 1 Let $\bar{\mathbf{P}}_\sigma = \mathbf{R}^{-\frac{1}{2}} \mathbf{P}_\sigma \mathbf{R}^{\frac{1}{2}}$, giving a positive definite matrix \mathbf{P}_σ , positive constants α , λ and $c_2/c_1 > 1$, the continuous time system is finite-time stabilized when the dwell time τ_α for each subsystem satisfies the ADT

condition (23), and the switching controllers can be constructed by solving linear matrix inequations (LMIs) (21) and (22).

$$\begin{bmatrix} \mathbf{A}_\rho^\top \bar{\mathbf{P}}_\sigma^{-1} + \bar{\mathbf{P}}_\sigma^{-1} \mathbf{A}_\rho - \lambda \bar{\mathbf{P}}_\sigma^{-1} & \sqrt{2\alpha} \bar{\mathbf{P}}_\sigma^{-1} \mathbf{B}_\rho \\ \sqrt{2\alpha} \mathbf{B}_\sigma^\top \bar{\mathbf{P}}_\rho^{-1} & -\mathbf{I} \end{bmatrix} \leq 0 \quad (21)$$

$$\frac{c_1}{\lambda_2} < \frac{c_2}{\lambda_1} e^{-\lambda T_f} \quad (22)$$

where

$$\begin{cases} \lambda_1 = \max_{\forall \sigma \in N} (\lambda_{\max}(\mathbf{P}_\sigma)) \\ \lambda_2 = \min_{\forall \sigma \in N} (\lambda_{\min}(\mathbf{P}_\sigma)) \end{cases}.$$

The controller gain is $\bar{\mathbf{K}}_{\sigma(t)} = \alpha \mathbf{B}_\rho^\top \bar{\mathbf{P}}_\sigma^{-1} \mathbf{x}$.

The ADT condition is

$$\tau_\alpha > \tau_\alpha^* = \frac{T_f \ln \left(\frac{\lambda_1}{\lambda_2} \right)}{\ln \left(\frac{c_2}{c_1} \right) - \ln \left(\frac{\lambda_1}{\lambda_2} \right) - \lambda T_f}. \quad (23)$$

Remark 4 In the design process of the tilt-rotor switching control, to guarantee the ADT condition, the dwell time should be limited within the transition time between adjacent command points, through adjusting control parameters. This procedure will be discussed in the simulation section.

Proof Construct the piecewise Lyapunov function as

$$v(t) = V_\sigma(\mathbf{x}) = \mathbf{x}^\top \bar{\mathbf{P}}_\sigma^{-1} \mathbf{x}. \quad (24)$$

When the aircraft subsystem is activated by the switching signal $\sigma(t)$, (25) can be derived.

$$\begin{aligned} \dot{V}_\sigma(\mathbf{x}) &= \mathbf{x}^\top \bar{\mathbf{P}}_\sigma^{-1} (\mathbf{A}_\rho \mathbf{x} + \mathbf{B}_\rho \bar{\mathbf{u}}) + (\mathbf{A}_\rho \mathbf{x} + \mathbf{B}_\rho \bar{\mathbf{u}})^\top \bar{\mathbf{P}}_\sigma^{-1} \mathbf{x} = \\ & \mathbf{x}^\top (\mathbf{A}_\rho^\top \bar{\mathbf{P}}_\sigma^{-1} + \bar{\mathbf{P}}_\sigma^{-1} \mathbf{A}_\rho) \mathbf{x} + \\ & \mathbf{x}^\top \bar{\mathbf{P}}_\sigma^{-1} \mathbf{B}_\rho \bar{\mathbf{u}} + \bar{\mathbf{u}}^\top \mathbf{B}_\rho^\top \bar{\mathbf{P}}_\sigma^{-1} \mathbf{x} \end{aligned} \quad (25)$$

When it satisfies the following condition (26), $\dot{V}_\sigma(\mathbf{x})$ can be expressed as (27).

$$\mathbf{A}_\rho \bar{\mathbf{P}}_\sigma^{-1} + \bar{\mathbf{P}}_\sigma^{-1} \mathbf{A}_\rho + 2\alpha \bar{\mathbf{P}}_\sigma^{-1} \mathbf{B}_\rho \mathbf{B}_\rho^\top \bar{\mathbf{P}}_\sigma^{-1} - \lambda \bar{\mathbf{P}}_\sigma^{-1} < 0 \quad (26)$$

$$\begin{aligned} \dot{V}_\sigma(\mathbf{x}) &= \mathbf{x}^\top (\mathbf{A}_\rho^\top \bar{\mathbf{P}}_\sigma^{-1} + \bar{\mathbf{P}}_\sigma^{-1} \mathbf{A}_\rho) \mathbf{x} + \\ & \mathbf{x}^\top \bar{\mathbf{P}}_\sigma^{-1} \mathbf{B}_\rho \alpha \mathbf{B}_\rho^\top \bar{\mathbf{P}}_\sigma^{-1} \mathbf{x} + \alpha \mathbf{x}^\top \bar{\mathbf{P}}_\sigma^{-1} \mathbf{B}_\rho \mathbf{B}_\rho^\top \bar{\mathbf{P}}_\sigma^{-1} \mathbf{x} = \\ & \mathbf{x}^\top (\mathbf{A}_\rho^\top \bar{\mathbf{P}}_\sigma^{-1} + \bar{\mathbf{P}}_\sigma^{-1} \mathbf{A}_\rho + 2\alpha \bar{\mathbf{P}}_\sigma^{-1} \mathbf{B}_\rho \mathbf{B}_\rho^\top \bar{\mathbf{P}}_\sigma^{-1}) \mathbf{x} < \\ & \lambda \mathbf{x}^\top \bar{\mathbf{P}}_\sigma^{-1} \mathbf{x} = \lambda V_\sigma(\mathbf{x}) \end{aligned} \quad (27)$$

It should be noted that Matlab/LMI toolbox cannot solve the inequality constraint (26) directly, so we transform the condition into (28) by the Schur theorem.

$$\begin{bmatrix} \mathbf{A}_\rho^\top \bar{\mathbf{P}}_\sigma^{-1} + \bar{\mathbf{P}}_\sigma^{-1} \mathbf{A}_\rho - \lambda \bar{\mathbf{P}}_\sigma^{-1} & \sqrt{2\alpha} \bar{\mathbf{P}}_\sigma^{-1} \mathbf{B}_\rho \\ \sqrt{2\alpha} \mathbf{B}_\sigma^\top \bar{\mathbf{P}}_\rho^{-1} & -\mathbf{I} \end{bmatrix} \leq 0 \quad (28)$$

In the tilt-rotor aircraft system, the transition initial time $T_0 = 0$.

Thus the piecewise Lyapunov function is

$$\begin{aligned} V(t) &\leq V(t_k) e^{\lambda(t-t_k)} \leq \\ & \frac{\lambda_1}{\lambda_2} [V(t_{k-1}) e^{\lambda(t_k-t_{k-1})}] e^{\lambda(t-t_k)} \leq \dots \leq \\ & \left(\frac{\lambda_1}{\lambda_2} \right)^{N_\sigma(0, T_f)} e^{\lambda t} V(0). \end{aligned} \quad (29)$$

Defining the initial switching time as $N_0 = 0$, the switching time satisfies $N_\sigma(0, T_f) \leq \frac{T(0, T_f)}{\tau_\alpha}$, thus

$$V(t) \leq \left(\frac{\lambda_1}{\lambda_2} \right)^{\frac{T(0, T_f)}{\tau_\alpha}} e^{\lambda t} V(0). \quad (30)$$

Due to the definition of λ_1 and λ_2 , we have (31) and (32).

$$V(t) = \mathbf{x}^\top \bar{\mathbf{P}}_\sigma^{-1} \mathbf{x} \geq \lambda_{\min}(\bar{\mathbf{P}}_\sigma^{-1}) \mathbf{x}^\top \mathbf{R} \mathbf{x} \geq \frac{1}{\lambda_1} \mathbf{x}^\top \mathbf{R} \mathbf{x} \quad (31)$$

$$V(0) = \mathbf{x}^\top(0) \bar{\mathbf{P}}_\sigma^{-1} \mathbf{x}(0) \leq \lambda_{\max}(\bar{\mathbf{P}}_\sigma^{-1}) \mathbf{x}^\top(0) \mathbf{R} \mathbf{x}(0) \leq \frac{1}{\lambda_2} \mathbf{x}^\top(0) \mathbf{R} \mathbf{x}(0) \quad (32)$$

It can be derived that

$$\begin{aligned} \mathbf{x}^\top \mathbf{R} \mathbf{x} &\leq \lambda_1 V(t) < \\ & \lambda_1 \left(\frac{\lambda_1}{\lambda_2} \right)^{\frac{T(0, T_f)}{\tau_\alpha}} e^{\lambda t} V(0) \leq \\ & \left(\frac{\lambda_1}{\lambda_2} \right) \cdot \left(\frac{\lambda_1}{\lambda_2} \right)^{\frac{T(0, T_f)}{\tau_\alpha}} e^{\lambda t} \mathbf{x}^\top(0) \mathbf{R} \mathbf{x}(0) = \\ & \left(\frac{\lambda_1}{\lambda_2} \right)^{\frac{T(0, T_f)}{\tau_\alpha} + 1} e^{\lambda t} \mathbf{x}^\top(0) \mathbf{R} \mathbf{x}(0). \end{aligned} \quad (33)$$

According to (22), we can obtain

$$\ln \left(\frac{c_2}{c_1} \right) - \ln \left(\frac{\lambda_1}{\lambda_2} \right) - \lambda T_f > 0. \quad (34)$$

Thus (34) can be written as

$$\begin{aligned} \mathbf{x}^\top \mathbf{R} \mathbf{x} &< \frac{c_2}{c_1} e^{\lambda t} e^{-\lambda t} \mathbf{x}^\top(0) \mathbf{R} \mathbf{x}(0) \leq \\ & \frac{c_2}{c_1} \mathbf{x}^\top(0) \mathbf{R} \mathbf{x}(0) \leq c_2. \end{aligned} \quad (35)$$

It implies the system is finite time stable as long as the state trajectory is continuous in $[0, T_f]$. \square

In this paper, to reduce the state vibrations and bumps in the switching point, the fuzzy weighted strategy is employed as a measure of ‘smoothness’ for switching. Due to the fact that the tilt-rotor aircraft transits along the previously known conversion path, this paper employs the fuzzy weighted strategy to schedule the controller, the smooth control signals can be expressed as

$$\bar{u}^* = \sum_{\rho=1}^N h_{\rho} \bar{K}_{\sigma(t)} x \quad (36)$$

where $h_{\rho} \geq 0$, $\sum_{\rho=1}^N h_{\rho} = 1$.

Without loss of generality, this study takes nacelle tilting from 65° to 45° as an example to illustrate the control design process. The flight speed and nacelle angle, which determine the flight mode along the conversion corridor, are chosen as the fuzzy inputs to estimate the current plant dynamic. The fuzzy segmentations are given as below.

(i) Input1 (V): fuzzy set = $[V_1, V_2, V_3]$, denotes states of flight velocities.

(ii) Input2 (β_M): fuzzy set = $[\beta_{M1}, \beta_{M2}, \beta_{M3}]$, denotes states of the nacelle angle.

(iii) Output (MD): fuzzy set = $[MD_1, MD_2, MD_3]$, corresponds to three flight modes.

The degree of membership is shown as Fig. 5.

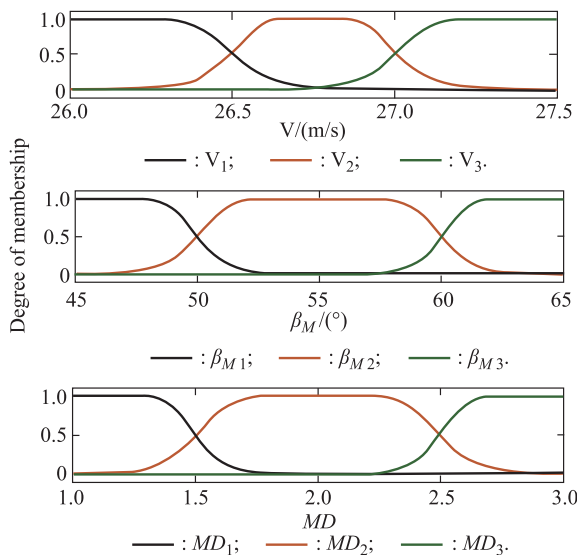


Fig. 5 Membership function

Remark 5 The fuzzy rules and fuzzy segmentation are designed according to the conversion path.

The center-of-area method is employed for the defuzzification, and the corresponding result is shown as Fig. 6.

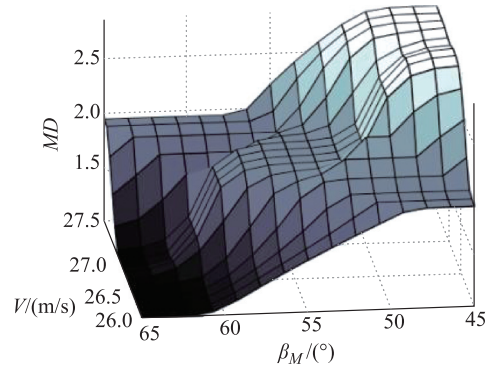


Fig. 6 Fuzzy weighted surface

Thus, the weight coefficients h_{ρ} can be described as

$$\begin{cases} h_{\rho} = 1 - |MD - \rho| \\ \rho = 1, 2, \dots, N \end{cases} \quad (37)$$

4. Simulations and analysis

To demonstrate the effectiveness of the control law, three typical tilt-rotor aircraft working points are taken as an example (with nacelle angles of 45° , 55° , 65°) and the references of the command points are trimmed as Table 2.

Table 2 Trim points at transition mode

Nacelle angle $\beta_M/(^{\circ})$	Forward speed $V_x/(m/s)$	Vertical speed $V_y/(m/s)$	Pitch rate $\omega/(^{\circ})/s$	Pitch angle $\theta/(^{\circ})$
65	26.25	0	0	3.7
55	26.75	0	0	3.7
45	27.25	0	0	3.5

It is worth noting that all these simulations are performed on the nonlinear model. The transition parameters and the simulation results are given respectively to prove that the system has good characteristics of smoothness and robustness.

The scheduling rule for the nacelle angle can be described as

$$\begin{cases} \beta_M = \beta_{M_0} + \left(\frac{\beta_{M_f} - \beta_{M_0}}{T_f} \right) t \\ \ddot{\beta}_M = 0 \end{cases} \quad (38)$$

where $T_0 \leq t \leq T_f$.

As is shown in (38), the aircraft tilting from 65° to 45° is described as a constant rotation process with the conversion time of 4 s.

Remark 6 In [35], the whole tilting process of the nacelle can be divided into three stages: initial acceleration stage, tilting in a constant speed, slowing down to stop. This simulation concentrates on the second stage.

It should be noted that, not only the tilting process, but also the selection of the matrix R has a close relation with

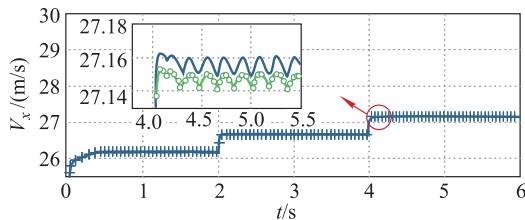
the transition performance, which can be shown as below. (In R selection, to clearly observe the system performances after the last switching, the aircraft keeps in 45° for 2 s (from 4 s to 6 s)).

As can be seen from Table 3, the selection of the matrix R has a close relation with the system dynamic performance and ADT. ADT needs to be shortened within the transition time of adjacent points, so the switching time is chosen as $t = 2$ s. The results are shown as below.

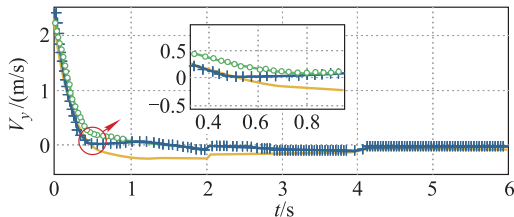
Table 3 Relation between R and ADT

Matrix R	λ_1/λ_2	ADT/s
diag ([40,25,48,97])	5.513 2	1.922 9
diag ([40,25,500,500])	1.877 3	0.544 3
diag ([40,25,1 000,1 000])	1.824 0	0.516 2

As can be seen from Table 3 and Fig. 7, the control system with a larger matrix R has a shorter ADT time, but worse dynamic performance.



(a) Forward speed response



(b) Vertical speed response

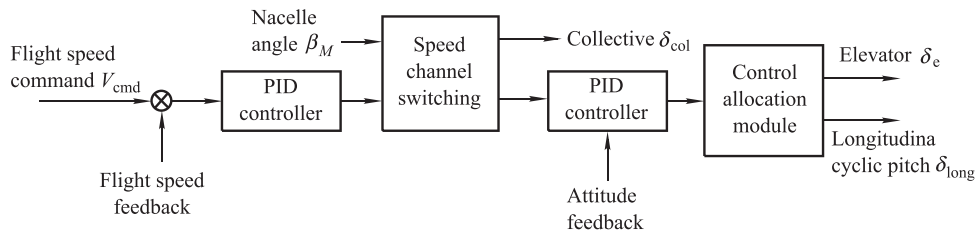
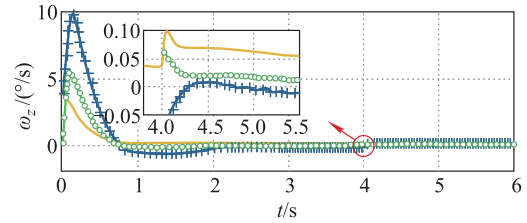


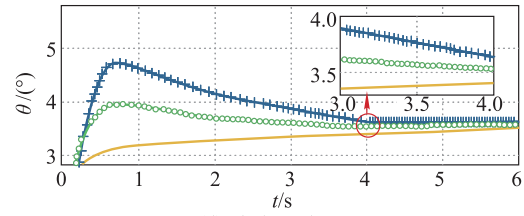
Fig. 8 Structure of PID control

The corresponding simulation results are shown in Fig. 9 and Fig. 10.

As is shown above, due to the huge variation of aerodynamic characteristics, the traditional PID control, which only uses one set of parameters in the transition process, is hard to satisfy the requirement of control precision. Due to the changeable dynamics of the tilt-rotor, a single con-



(c) Pitch rate response



(d) Pitch angle response

—: $R=\text{diag}[40\ 25\ 1\ 000\ 1\ 000]$; —+—: $R=\text{diag}[40\ 25\ 48\ 97]$;
—o—: $R=\text{diag}[40\ 25\ 500\ 500]$.

Fig. 7 Flight states under different R

For the purpose of altitude maintenance, the pitch angle should track the command signal in a short time; otherwise, the lack of pitch angle makes the wing unable to provide enough lift force to balance the rotor thrust loss in the vertical direction, which will make the altitude fall.

Thus, we adjust the parameter of the controller as: $R = \text{diag}([40, 25, 48, 97])$, $\alpha = 0.79$, $\lambda = 0.01$, $c_2/c_1 = 200$.

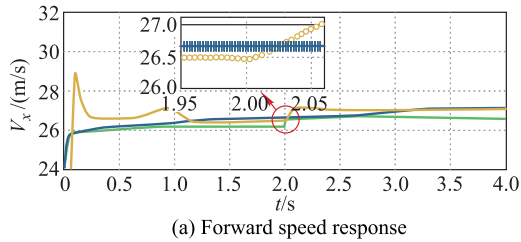
The classic PID is common for the tilt-rotor aircraft in control design. To show the design difference and system performance between PID and the proposed method, this paper makes a simple comparison.

The control structure of PID is shown as Fig. 8. The control allocation strategy and the control channel switching strategy are both employed to solve the problem of the control surface redundancy. We will not cover the details of them here.

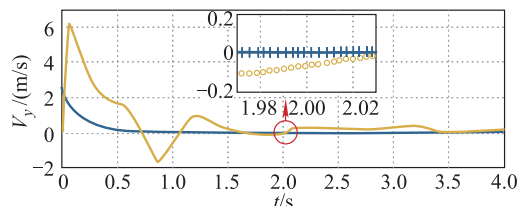
troller does not work very well either. In addition, when PID controls the tilt-rotor aircraft with the characteristic of multivariable, strong coupling and control surface redundancy, the control channel switching strategy should also be considered, which further increases the complexity of the design.

Compared with switching directly, the smooth switching

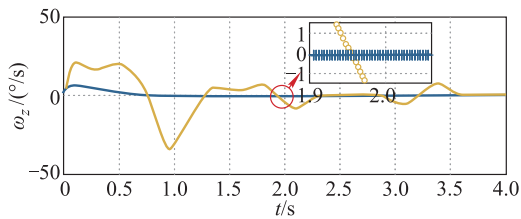
by the fuzzy weighted strategy reduces the states vibrations and bumps at the switching point. Meanwhile, the smooth switching scheme also reduces the jumps of the control signal. Thus, the proposed smooth switching method enhances the transient performance in the transition process.



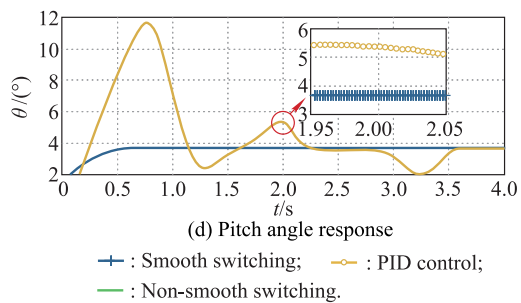
(a) Forward speed response



(b) Vertical speed response

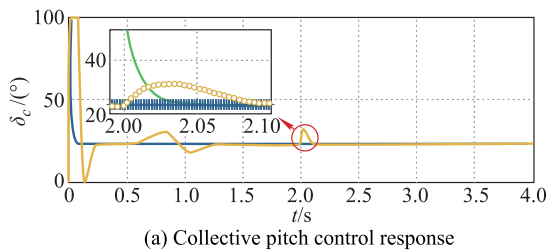


(c) Pitch rate response

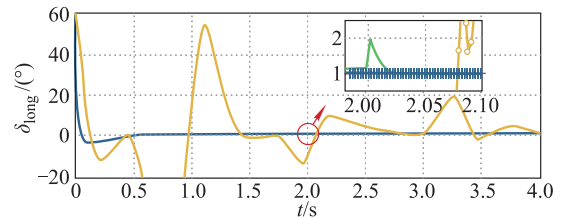


(d) Pitch angle response
 + : Smooth switching; - : PID control;
 - : Non-smooth switching.

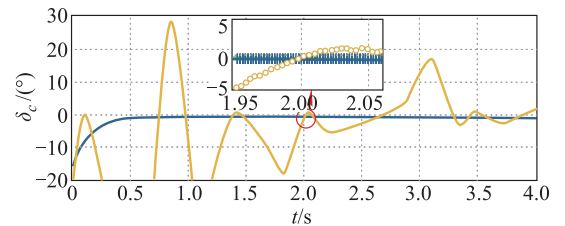
Fig. 9 System states responses



(a) Collective pitch control response



(b) Longitudinal cyclic pitch response



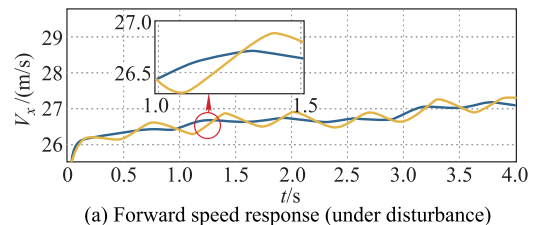
(c) Elevator control response

+ : Smooth switching; - : PID control;
 - : Non-smooth switching.

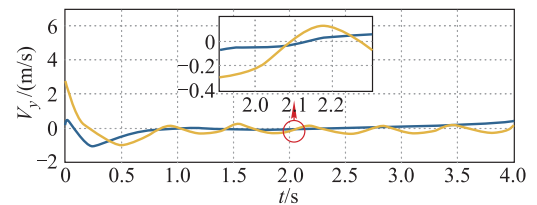
Fig. 10 System control responses

To further validate the robustness of the proposed method, the external sinusoidal interference signal d (with the amplitude of 15 and the frequency of 10) is respectively added to the forward speed V_x , the vertical speed V_y , and the pitch rate ω_z .

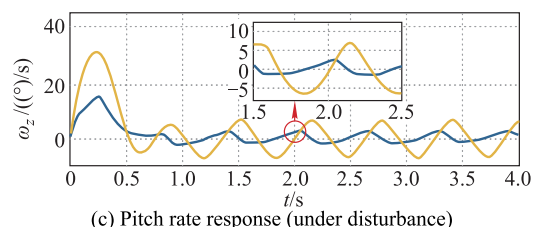
The following simulations compare two systems, one applying the smooth switching controller with ESO, and the other applying the smooth switching controller without ESO. The corresponding results are shown in Fig. 11.



(a) Forward speed response (under disturbance)



(b) Vertical speed response (under disturbance)



(c) Pitch rate response (under disturbance)

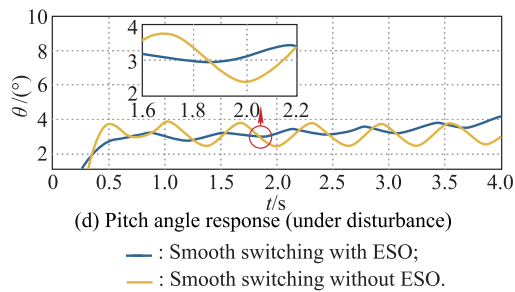


Fig. 11 System states responses (under disturbance)

As can be seen from Fig. 11, without applying the ESO to smooth switching control, the disturbance fluctuation to V_x is reduced to 1.11% of the initial interference amplitude, V_y to 11.1%, ω_z to 8.6%, which illustrates that the smooth switching control method (without ESO) has a certain degree of robustness. However, applying ESO to compensating for the disturbance, the disturbance to V_x can be furthered to 0.22% of the initial interference amplitude, V_y to 1.19%, ω_z to 2.9%.

The two results show that the ESO based system has a better disturbance rejection ability, which could lead to a better response. The system robustness can be further analyzed that, the switching parameters gradually change along the conversion trajectory, which suggests that the state matrix of each subsystem is perturbed actually. However, it can be seen from the above figures that, although there exists both external disturbance and parameter perturbation in the system, the transition is stable. This result further supports the conclusion that the proposed control can achieve better results with a strong robustness.

5. Conclusions

The flight dynamic of a tilt-rotor aircraft is much more complex than the traditional aircraft, because its configuration changes by tilting.

Based on its characteristic of violent aerodynamic parameter variation, the smooth switching control scheme is designed to deal with the complex flight dynamics problem. Furthermore, to diminish the influence of disturbance, the proposed control structure combines the ESO and the model information-based control strategy.

The simulation comparison between the classic PID and the proposed method demonstrates that, for the tilt-rotor aircraft, the new smooth switching control scheme is more targeted and superior to the traditional design method.

References

- [1] KIM B M, CHOI K C, KIM B S. Trajectory tracking controller design using neural networks for tiltrotor UAV. Proc. of the AIAA Guidance, Navigation & Control Conference & Exhibit, 2007: 1–15.
- [2] XIA Q Y, XU J F, ZHANG L. Model free adaptive attitude controller for a tilt-rotor aircraft. Systems Engineering and Electronics, 2013, 35(1): 146–151. (in Chinese)
- [3] SONG S, WANG W, LU K, et al. Nonlinear attitude control using extended state observer for tilt-rotor aircraft. Proc. of the 27th Control and Decision Conference, 2015: 852–857.
- [4] SONG Y G, WANG H J. Design of flight control system for a small unmanned tilt rotor aircraft. Chinese Journal of Aeronautics, 2009, 22(3): 250–256.
- [5] KIM B M, KIM B S, KIM N W. Trajectory tracking controller design using neural networks for a tiltrotor unmanned aerial vehicle. Proc. of the Institution of Mechanical Engineers Part G: Journal of Aerospace Engineering, 2010, 224(G8): 881–896.
- [6] ZHANG J, SUN L G, QU X J, et al. Time-varying linear control for tiltrotor aircraft. Chinese Journal of Aeronautics, 2018, 31(4): 632–642.
- [7] WANG Q, WU W H, QING D B. A nonlinear adaptive switching control blending method and its application to tiltrotor. Acta Aeronautica Et Astronautica Sinica, 2015, 36(10): 3359–3369. (in Chinese)
- [8] RUGH W J, SHAMMA J S. Research on gain scheduling. Automatica, 2000, 36(10): 1401–1425.
- [9] YEO Y T, LIU H H T. Transition control of a tilt-rotor VTOL UAV. Proc. of the AIAA Guidance, Navigation, and Control Conference, 2018: 1–15.
- [10] KONG Z W, LU Q. Mathematical modeling and modal switching control of a novel tiltrotor UAV. Journal of Robotics, 2018, 2018: 8641731.
- [11] TURNER M C, AOUF N, BATES D G, et al. A switching scheme for full-envelope control of a V/STOL aircraft using LQ bumpless transfer. Proc. of the International Conference on Control Applications, 2002: 120–125.
- [12] KUIPERS M, LOANNOUS P. Multiple model adaptive control with mixing. IEEE Trans. on Automatic Control, 2010, 55(8): 1822–1836.
- [13] BALDI S, IOANNOU P A, KOSMATOPOULOS E B. Adaptive mixing control with multiple estimators. International Journal of Adaptive Control and Signal Processing, 2012, 26(8): 800–820.
- [14] MANIMALA B, PADFIELD G D, WALKER D. Load alleviation in tilt rotor aircraft through active control; modelling and control concepts. The Aeronautical Journal, 2004, 108(1082): 169–184.
- [15] SUN Z, WANG R, ZHOU W Y. Finite-time stabilization control for the flight mode transition of tiltrotors based on switching method. Proc. of the 29th Chinese Control and Decision Conference, 2017: 2049–2053.
- [16] LU L H, FU R, ZENG J P. Mode conversion of electric tilt rotor aircraft based on corrected generalized corridor. Acta Aeronautica Et Astronautica Sinica, 2018, 39(8): 121900. (in Chinese)
- [17] ZHAO Y, MA D, ZHAO J. Almost output regulation bumpless transfer control for switched linear systems. IET Control Theory and Applications, 2018, 12(14): 1932–1940.
- [18] KHANI F, HAERI M. Smooth switching in a scheduled robust model predictive controller. Journal of Process Control, 2015, 31: 55–63.
- [19] HE T Y, ZHU G M G, SWEI S S M, et al. Smooth-switching LPV control for vibration suppression of a flexible airplane wing. Aerospace Science and Technology, 2019, 84: 895–903.
- [20] CHENG H Y, DONG C Y, WANG Q, et al. Smooth switching linear parameter-varying fault detection filter design for morphing aircraft with asynchronous switching. Transactions of

- the Institute of Measurement and Control, 2018, 40(8): 2622–2638.
- [21] MALLOCI L, HETEL L, DAAFOUZ J, et al. Bumpless transfer for switched linear systems. *Automatica*, 2012, 48(7): 1440–1446.
- [22] TURNER M C, WALKER D J. Linear quadratic bumpless transfer. *Automatica*, 2000, 36(8): 1089–1101.
- [23] JIANG W L, DONG C Y, WANG Q. A systematic method of smooth switching LPV controllers design for a morphing aircraft. *Chinese Journal of Aeronautics*, 2015, 28(6): 1640–1649.
- [24] JIANG W L, DONG C Y, WANG T, et al. Smooth switching LPV robust control for morphing aircraft. *Control and Decision*, 2016, 31(1): 66–72. (in Chinese)
- [25] GAO Z Q. Active disturbance rejection control: a paradigm shift in feedback control system design. *Proc. of the American Control Conference*, 2006: 2399–2405.
- [26] HAN J Q. From PID to active disturbance rejection control. *IEEE Trans. on Industrial Electronics*, 2009, 56(3): 900–906.
- [27] GUO J D, SONG Y G, XIA P Q. Full envelope flight control method for small unmanned tilt rotor aircraft. *Journal of Nanjing University of Aeronautics & Astronautics*, 2009, 41(4): 439–444. (in Chinese)
- [28] GUO J D. Flight control of unmanned tiltrotor aircraft. Nanjing, China: Nanjing University of Aeronautics and Astronautics, 2013. (in Chinese)
- [29] CAO Y Y. Research on mathematical modeling method for tilt-rotor aircraft flight dynamics. Nanjing, China: Nanjing University of Aeronautics and Astronautics, 2012. (in Chinese)
- [30] KLENHESSELINK K M. Stability and control modeling of tilt-rotor aircraft dynamics. Maryland, USA: University of Maryland, 2007.
- [31] YANG J, WU X M, FAN Y H. Flight control of the tilt-rotor aircraft. Beijing: Aviation Industry Press, 2006. (in Chinese)
- [32] ZHANG G L, YANG L Y, JING Z, et al. Longitudinal attitude controller design for aircraft landing with disturbance using ADRC/LQR. *Proc. of the IEEE International Conference on Automation Science & Engineering*, 2013: 330–335.
- [33] AMATO F, ARIOLA M, DORATO P. Finite-time control of

linear systems subject to parametric uncertainties and disturbances. *Automatica*, 2001, 37(9): 1459–1463.

- [34] HESPANHA J P, MORSE A S. Stability of switched systems with average dwell-time. *Proc. of the 38th IEEE Conference on Decision and Control*, 1999: 2655–2660.
- [35] LAI S Q, YAN F, XU K. Design and research of control law for tiltrotor in transition flight phase. *Helicopter Technique*, 2009, 159(3): 52–55. (in Chinese)

Biographies



ZOU Yiru was born in 1994. She is a master candidate in navigation, guidance and control in Nanjing University of Aeronautics and Astronautics. Her research interests are flight control, especially V/STOL aircraft control, switching control and active disturbance rejection control.
E-mail: zouyiru427@163.com



LIU Chunsheng was born in 1955. She is a Ph.D. and a professor in Nanjing University of Aeronautics and Astronautics. Her research interests are adaptive robust control of nonlinear system, fault-tolerant control and intelligent control.
E-mail: liuchsh@nuaa.edu.cn



LU Ke was born in 1985. He is a Ph.D. candidate in Nanjing University of Aeronautics and Astronautics and also a senior engineer in China Helicopter Research and Development Institute. His research interests are flight dynamics, flight aerodynamic modeling and flight control.
E-mail: looknuaa@163.com